Continuous loading of $^1S_0$ calcium atoms into an optical dipole trap

C. Y. Yang, P. Halder, O. Appel, D. Hansen, and A. Hemmerich
Institut für Laser-Physik, Universität Hamburg, Luruper Chaussee 149, 22761 Hamburg, Germany
(Received 5 June 2007; published 28 September 2007)

We demonstrate an efficient scheme for continuous trap loading based upon spatially selective optical pumping. We discuss the case of $^1S_0$ calcium atoms in an optical dipole trap (ODT), however, similar strategies should be applicable to a wide range of atomic species, which do not permit efficient conventional trap loading. Our starting point is a moderately cold ($\approx 300\ \mu$K) and dense ($\approx 9\times 10^9$ cm^{-3}) reservoir of metastable $^3P_2$ atoms in a magneto-optic trap (triplet MOT). A focused 532 nm laser beam produces a strongly elongated optical potential for $^1S_0$ atoms with up to 350 μK well depth. A weak focused laser beam at 430 nm, carefully superimposed upon the ODT beam, selectively pumps the $^3P_2$ atoms inside the capture volume to the singlet state, where they are confined by the ODT. The triplet MOT perpetually refills the capture volume with $^3P_2$ atoms, thus providing a continuous stream of cold atoms into the ODT at a rate of 10^7 s^{-1}. Limited by evaporation loss, in 200 ms we typically load 5×10^5 atoms with 3.5×10^{10} cm^{-3} peak density and axial and radial temperatures of 300 and 85 μK, respectively. After terminating the loading we observe evaporation during 50 ms, typically leaving us with 10^5 atoms with nearly equal radial and axial temperatures close to 40 μK and a peak density of 5×10^{11} cm^{-3}. A simple model is presented, which identifies the relevant physical mechanisms of the loading and decay dynamics. We point out that a comparable scheme could be employed to load a dipole trap with $^3P_0$ atoms.

DOI: 10.1103/PhysRevA.76.033418 PACS number(s): 32.80.Pj, 34.50.−s, 82.20.Pm

The unique spectroscopic features of two-electron systems and their usefulness for the fields of time metrology [1], cold collision physics [2,3], and quantum gases [4] has led to extensive efforts to improve laser cooling and trapping techniques for alkaline-earth-metal (AEM) atoms [5–12]. Calcium is a particularly interesting example, because, aside from its excellent performance in optical atomic clock scenarios [13,14], its singlet ground state (in contrast to the most abundant strontium isotope [15]) has a large positive scattering length with favorable prospects for reaching quantum degeneracy [16]. Optical trapping is a key technique in modern atomic physics, indispensable in numerous recent experiments with ultracold atoms and molecules [17]. In particular, if magnetic trapping techniques fail to work, as in the singlet manifold of the AEM group, optical dipole traps (ODTs) practically have no alternative.

ODTs typically provide good compression, but suffer from limited trap depths of several hundred μK, owing to limitations in available laser powers. Thus, efficient loading of ODTs typically requires a magneto-optic trap (MOT) permitting sufficiently low temperatures well below 100 μK, which is not always available. Although magneto-optical trapping of AEM-like atoms in the ground state is in fact possible using their principal fluorescence lines, the attainable temperatures of several mK are too high for efficient direct loading of an ODT. In some cases, e.g. for strontium or ytterbium, additional cooling by means of intercombination lines [5,10] have been used for ODT loading with large phase space densities. Unfortunately, this does not likewise apply to magnesium or calcium, because of the low bandwidths of their intercombination lines, although low temperatures were reported in the case of calcium [6,7].

In this article we investigate an efficient loading technique for an ODT of calcium atoms in the singlet ground state $^1S_0$. Our approach has some similarities with a technique originally proposed and experimentally demonstrated for the loading of optical surface traps [18]. We are also aware of a brief note in Ref. [19] that a related technique has been recently used to trap strontium atoms with a capture rate of 10^5 s^{-1}. We start with a moderately cold ($\approx 300\ \mu$K) and dense ($\approx 9\times 10^9$ cm^{-3}) sample of metastable $^3P_2$ atoms in a magneto-optic trap (triplet MOT) using infrared radiation at 1978 nm. This MOT is loaded by a conventional MOT for $^1S_0$ atoms (singlet MOT), operating on the principle fluorescence line at 423 nm (for details see Refs. [8,9]). A linearly polarized, focused laser beam ($1/e^2$ radius: $w_0=22.5\ \mu$m, confocal parameter: $b=w_0^2 2\pi/\lambda \approx 6$ mm) at $\lambda=532$ nm with up to 3 W power produces a tight, strongly elongated, horizontally oriented light shift potential for $^1S_0$ atoms with up to 350 μK well depth. Negative light shifts also arise for the $^3P_2$ and the $^3P_1$ levels [cf. Fig. 1(b)]. Atoms are loaded into the ODT by optical pumping using a weak violet laser beam at 430 nm with a $1/e^2$ beam radius $w_1=17\ \mu$m. This beam resonantly excites the $[4s4p]^3P_2$ atoms to $[4p^2]^3P_2$ from where they may decay to the singlet ground state via $[4s4p]^3P_1$ [cf. Fig. 1(c)]. As sketched in Fig. 1(d), the optical pumping beam is shaped to match the ODT potential, such that only $^3P_2$ atoms located within the capture volume are pumped to the light shift potential of the $[4s4p]^3P_1$ level and further decay to the $^1S_0$ ODT within 0.42 ms. The capture volume perpetually refills with $^3P_2$ atoms from the triplet MOT, i.e., a continuous stream of cold atoms is transferred to the ODT. The population of the ODT exponentially approaches a steady state determined by the balance between loading and evaporation loss, long before the $^3P_2$ population of the triplet MOT of several 10^8 atoms is exhausted. We obtain excellent capture rates of up to 10^7 s^{-1}. In steady state, this yields typically 5×10^5 trapped atoms with a peak density of 3.5×10^{10} cm^{-3} and with different axial and radial temperatures of 300 and 85 μK. After terminating the loading we observe evaporation during 50 ms typically leaving us with 10^5 atoms at a temperature of 42 μK and a peak

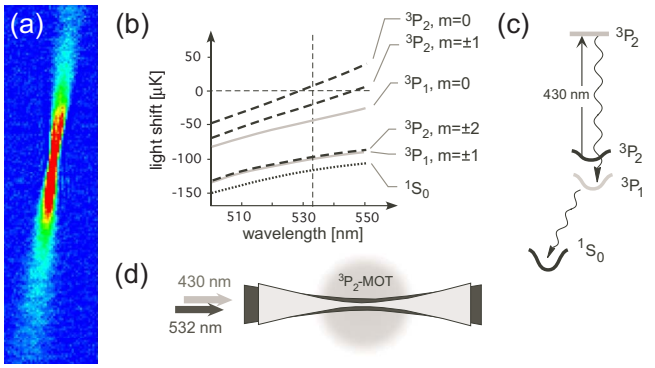

FIG. 1. (Color online) (a) Absorption image of ODT. The line of sight encloses a small angle of 4° with the ODT beam. (b) Light shifts of the relevant levels for 1 W and π polarization. (c) Levels relevant for loading of ODT. (d) Geometry of the ODT and optical pumping beam.

density of 5.3×10^{11} cm^{-3}. This corresponds to a notable increase of the phase space density from 4.1×10^{-8} in the triplet MOT to 3.6×10^{-5} in the ODT, despite the extremely different ODT and MOT volumes, the relatively low trap depth, and the large sizes of the photon scattering cross section and the cross section for inelastic collisions between $[4s4p]^3P_2$ atoms [20], limiting the performance of the triplet MOT.

The exponential loading dynamics at varying optical pumping powers is studied as follows. After loading the triplet MOT for 1 s, the singlet MOT is extinguished and the ODT beam and the pumping beam are enabled. The negative frequency detuning of the triplet-MOT beams is increased to compensate for the negative light shift of the triplet-MOT transition within the capture volume, at the cost of an undesired increase of the triplet-MOT temperature to values around 300 μK. After a variable time, ODT loading is terminated and an absorption image is taken, which lets us derive the instantaneous number of atoms in the ODT. Typical examples of the observed exponential loading curves are plotted in Fig. 2(a). Such curves let us determine the number of atoms $\bar{N}$ loaded into the ODT in steady state [black triangles in Fig. 2(b)], the capture rate R [open circles in Fig. 2(b)], obtained as the initial slope of the exponential fits in Fig. 2(a) and the 1/e loading time τ [black squares in Fig. 2(c)]. For very low powers R increases with power yielding an increase of $\bar{N}$ and a decrease of τ. The increase of R arises because below saturation the optical pumping rate is proportional to the light intensity. The consequential increase of $\bar{N}$ yields an increase of the density in the ODT and thus an increase of evaporative loss, which in turn yields a decrease of τ. When saturation of the pumping transition is approached, the effective pumping volume begins to exceed the capture volume of the ODT, i.e., many triplet-MOT atoms are pumped outside this capture volume, which is less efficiently refilled. Thus, R decreases again for high pump powers, which should be accompanied by an increase of τ due to reduced evaporation. The observations in Fig. 2(c) indicate that for large pump powers an additional loss mechanism sets in, which keeps the value of τ smaller than expected

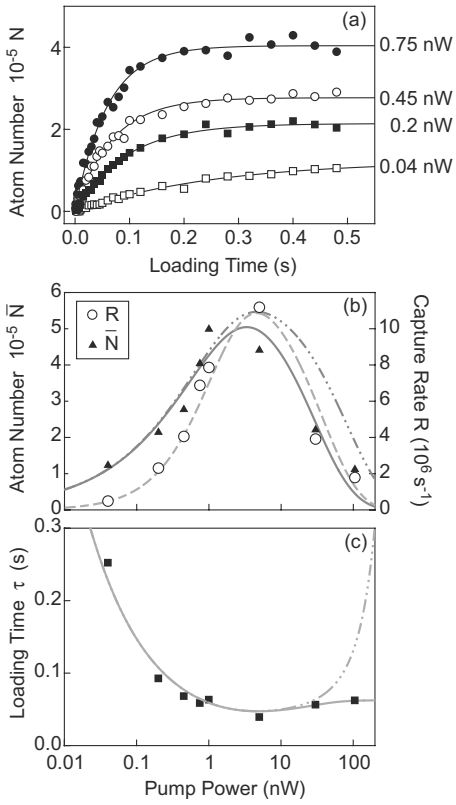

FIG. 2. In (a) trap loading measurements are shown for different values of the optical pumping power indicated on the right margin. The solid lines are exponential fits. (b) The black triangles show the measured steady-state number of atoms. The solid and the dashed-dotted lines depict the results of the model discussed in the text, if γ_B is included and if $\gamma_B=0$, respectively. The open circles show the measured capture rate with the respective calculations given by the dashed line. In (c) the 1/e loading time is plotted. The solid and the dashed-dotted lines show the calculations if γ_B is included and if $\gamma_B=0$, respectively.

from evaporation of the relatively small ODT population. Our theoretical analysis indicates that the increased populations of $^3P_1$ and $^1S_0$ atoms pumped outside the ODT capture volume act as an additional background introducing extra losses.

The preceding considerations can be rendered more precisely by extending a common model applied in numerous previous works [20,21,23]. The instantaneous number of $^1S_0$ atoms N in the ODT evolves according to

$$\frac{d}{dt}N = R(P) - [\gamma + \gamma_B(P)]N - \gamma_{ev}(T)N^2. \tag{1}$$

Here, γ is a loss rate, independent of the pumping power, which accounts for collisions with fast background gas atoms or atoms in the triplet MOT, $\gamma_{ev}(T)$ is a temperature-dependent two-body loss parameter accounting for evaporative loss via elastic binary collisions between trapped singlet atoms, and $R(P)$ is the effective capture rate of the ODT for singlet atoms. We also allow for an additional power-dependent loss rate $\gamma_B(P)$ accounting for collisions of $^1S_0$

atoms trapped in the ODT with $^1S_0$ and $^3P_1$ atoms, optically pumped outside the trap volume, when large pump powers are applied. The dependences of the capture rate $R(P)$ and the loss rate $\gamma_B(P)$ on the pump power P are obtained by calculating the optical pumping probabilities inside and outside the ODT volume V_{ODT}. In this calculation we consider ballistic trajectories $\xi(t)$ of the triplet MOT atoms entering V_{ODT} at t_{in} and leaving it at t_{out}. The assumption of the ballistic nature of the atomic motion appears well justified on the few tens of micron length scale given by the waist of the ODT beam. A typical triplet MOT atom with mean velocity $\bar{v}$ (according to its temperature of 300 μK) randomly scatters a few tens of infrared photons during the traverse through V_{ODT}, which yields a negligible change of $\bar{v}$. Integration of the optical pumping rate $\Gamma(P,\xi(t))$ along $\xi(t)$ yields the probability for a triplet-MOT atom to enter V_{ODT} without being optically pumped $\wp_{1,\xi}(P)=\exp[-\int_{-\infty}^{t_{\mathrm{in}}}\Gamma(P,\xi(t))dt]$ and the probability for an atom that has entered V_{ODT} to leave it unpumped $\wp_{2,\xi}(P)=\exp[-\int_{t_{\mathrm{in}}}^{t_{\mathrm{out}}}\Gamma(P,\xi(t))dt]$. Hence, the probability to get pumped inside V_{ODT} is $\wp_{\mathrm{in},\xi}(P)\equiv\wp_{1,\xi}(P)(1-\wp_{2,\xi}(P))$, while the probability to get pumped outside V_{ODT} is $\wp_{\mathrm{out},\xi}(P)\equiv 1-\wp_{1,\xi}(P)$. An average over trajectories and velocities according to the temperature of the triplet MOT yields corresponding average probabilities $\wp_{\mathrm{in}}(P)$ and $\wp_{\mathrm{out}}(P)$ and we write $R(P)=R_0\wp_{\mathrm{in}}(P)$ and $\gamma_B(P)=\gamma_{B,0}\wp_{\mathrm{out}}(P)$. For the optical pumping rate $\Gamma(P,\xi(t))$ a two-level expression is used with an average Clebsch-Gordan coefficient to account for the magnetic substructure of the $[4s4p]^3P_2\rightarrow[4p^2]^3P_2$ transition ([22]) in connection with the linear polarization of the pump radiation. The boundary of V_{ODT} in this calculation is defined by the condition that the ODT potential has 1/3 of its maximal depth. The P dependences of $\wp_{\mathrm{in}}(P)$ and $\wp_{\mathrm{out}}(P)$ turn out to be fairly insensitive to the details of this definition.

The evaporation loss parameter may be written as $\gamma_{\mathrm{ev}}(T)\equiv 0.5\gamma_{\mathrm{coll}}(T)P_{\mathrm{loss}}(T)$, where $P_{\mathrm{loss}}(T)$ is the fraction of collisions yielding evaporation. The elastic collision parameter is given by $\gamma_{\mathrm{coll}}(T)=\sigma(T)\bar{u}(T)/V_{\mathrm{eff}}(T)$, where $\bar{u}(T)\equiv 4\sqrt{k_BT/\pi m}$ is the mean relative velocity, $\sigma(T)$ is the elastic collision cross section and $V_{\mathrm{eff}}(T)\equiv N^2/\int n(r)^2d^3r$ is the effective trap volume with $n(r)$ denoting the density distribution of trapped atoms. For the modeling of $P_{\mathrm{loss}}(T)$ we employ a harmonic approximation of the ODT potential. In this case the principle of detailed balance [24] yields $P_{\mathrm{loss}}(T)\approx 0.5(\eta^2+2\eta+2)\exp(-\eta)$ where $\eta\equiv U_0/k_BT$ and U_0 is the potential well depth. In order to model the temperature dependence of the effective trap volume, one may be tempted to resort to the harmonic approximation of the ODT potential as well, yielding $V_{\mathrm{eff}}(T)=bw_0^2\sqrt{\pi^3/2\eta^3}$. Because the ODT potential rapidly opens up towards higher energies this approach would notably underestimate the trap volume. To account for this fact, we introduce a correction factor $\upsilon(T)$ writing $V_{\mathrm{eff}}(T)=bw_0^2\sqrt{\pi^3/2\eta^3}\upsilon(T)$. In the following, we assume that the elastic scattering cross section and the volume correction factor are temperature independent, i.e., $\sigma(T)=\sigma_0$ and $\upsilon(T)=\upsilon_0$. The modeling of $V_{\mathrm{eff}}(T)$ may be regarded as a crude approximation, however, although comparably simple, it is certainly more realistic than assuming a temperature-independent trap volume.

According to the previous considerations, Eq. (1) comprises the three constants $\gamma_{B,0}$, R_0, and σ_0/υ_0, which take the role of fit parameters. As fixed parameters we use a well depth of $U_0/k_B=350$ μK (resulting from measurements of the power and the focus of the ODT beam), a value $1/\gamma=15$ s and a temperature $T_0\equiv(T_{\mathrm{ax},0}+2T_{\mathrm{rad},0})/3=157$ μK resulting from the initial axial and radial temperatures $T_{\mathrm{ax},0}=300$ μK and $T_{\mathrm{rad},0}=85$ μK. The used radial temperature results from measurements described below. Its value well below that of the triplet MOT of about 300 μK reflects the fact that atoms with small radial velocities remain longer in the pumping beam and are thus more efficiently loaded, i.e., the loading process is energy selective with respect to the radial degrees of freedom. Due to the extreme aspect ratio of the ODT this does not equally apply to the axial direction. The large axial trap diameter prevents any energy selectivity of the loading process with regard to the axial degree of freedom, and the axial temperature $T_{\mathrm{ax},0}$ should be roughly given by the temperature of the triplet MOT of about 300 μK. A reliable experimental determination of $T_{\mathrm{ax},0}$ via time-of-flight measurements, similarly as for $T_{\mathrm{rad},0}$, is impeded by the large axial extension of the trap.

To compare our model with the observations, Eq. (1) is solved for constant temperature T_0 and fit parameters $\gamma_{B,0}$, R_0, and σ_0/υ_0, in order to find the 1/e loading time $\tau=1/\sqrt{(\gamma+\gamma_B)^2+4R\gamma_{\mathrm{ev}}}$ and the steady state particle number $\bar{N}=(1/\tau-\gamma-\gamma_B)/(2\gamma_{\mathrm{ev}})$ (see, e.g., Ref. [23]). First, we adjust R_0, in order to optimize the agreement with the observed capture rates [open circles in Fig. 2(b)]. This yields the dashed line in Fig. 2(b). In a second step, σ_0/υ_0 and $\gamma_{B,0}$ are adjusted to obtain the solid line in Fig. 2(c). Finally, the calculated steady state number of atoms $\bar{N}(P)$ is scaled by a constant factor 0.53 to match with the observed data, which yields the solid line in Fig. 2(b). We believe that this reflects a systematic error in the absolute calibration of our absorption imaging system used to measure $\bar{N}$.

Our loading model suggests the use of $\sigma_0/\upsilon_0=2.9\times10^{-16}$ m^2. A simple calculation shows that at the temperature T_0 the volume correction factor is $\upsilon_0\approx 10$ and, hence, $\sigma_0\approx 3\times10^{-15}$ m^2. This exceeds the s wave unitarity limit at T_0 by a factor of 9, thus indicating the inappropriateness of the s-wave approximation. Recent calculations and measurements have set boundaries for the s-wave scattering length a_{scat} between 340 and 800 a_0 (a_0=Bohr radius) [16]. A detailed model connecting a_{scat} to the scattering cross section is not available for $^1S_0$ calcium atoms. With the help of the value of σ_0 we may discuss the significance and size of $\gamma_B(P)$. In Fig. 2(b) and 2(c) we also plotted the model predictions for $\gamma_B(P)=0$ (dashed-dotted curves), showing that the essential features of the predictions are maintained and the inclusion of $\gamma_B(P)$ only gives a relevant contribution for pump powers above a few nW. For 100 nW, τ is practically given by $1/\gamma_B\approx 60$ ms. At such high pump powers, we may assume that most triplet-MOT atoms in a region by far exceeding the ODT volume are pumped to the $^3P_1$ state, thus yielding a density of $^3P_1$ atoms comparable to that prepared in the triplet MOT on the order of 10^{10} cm^{-3}. Furthermore, a background of untrapped $^1S_0$ atoms with comparable density $\rho_B=10^{10}$ cm^{-3} is produced by means of spontaneous decay.

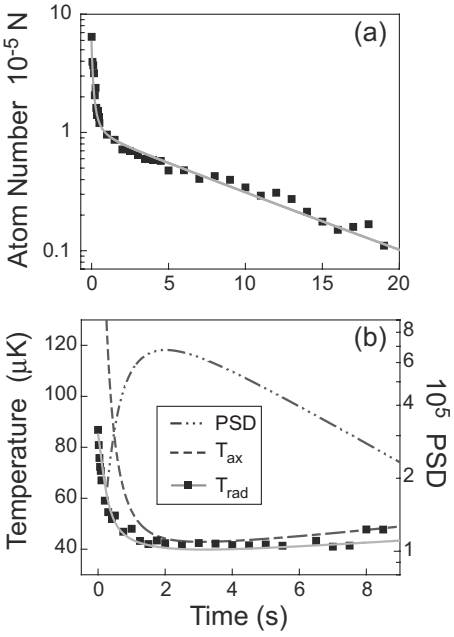

FIG. 3. The observed number of atoms [filled squares in (a)] and the radial temperature, [filled squares in (b)] are plotted versus time after loading is terminated. The gray lines are calculated with the model described in the text.

Assuming that each trapped $^1S_0$ atom colliding with an untrapped $^1S_0$ atom is lost, we may estimate $\gamma_B \approx \sigma_0 \rho_B \bar{u} \approx 15\ \mathrm{s}^{-1}$, where $\bar{u} \approx 50$ cm/s is the mean relative velocity between the atoms at 300 μK. This is in accordance with the 60 ms loading time shown in Fig. 2(c) for large pump powers. A similar consideration concerns the background of $^3P_1$ atoms, however, we do not know the scattering cross section for collisions between $^1S_0$ atoms and $^3P_1$ atoms. Finally, we can readily understand the power level of a few tenth of a nW at which loading becomes sizable according to Fig. 2. Assume a typical triplet-MOT atom with mean velocity $\bar{v}$ traversing the optical pumping beam [beam waist: w_1, peak optical pumping rate: $\Gamma_0(P)$] in a time $\tau_0 = w_1/\bar{v}$. Setting $\Gamma_0(P)\tau_0 = 1$ yields $P \approx 0.5$ nW.

We have also observed the time evolution of the particle number and the radial temperature of the ODT after loading is terminated. In these measurements the atoms are kept in the ODT for a variable time and subsequently a time-of-flight (TOF) method is applied. In the TOF procedure the ODT potential is switched off, the atoms are given the chance to expand ballistically for some period finished by taking an absorption image. A series of TOF measurements for a fixed hold-up time of the atoms in the ODT lets us derive the instantaneous radial temperatures and particle numbers. In Fig. 3 we have recorded the trap loss [filled squares in Fig. 3(a)] and the evolution of the radial temperature [filled squares in Fig. 3(b)] after loading is terminated. In Fig. 3(a) one recognizes a fast loss of atoms during the first 50 ms, which results from evaporation accompanied by a significant reduction of the initial radial temperature $T_{\mathrm{rad},0} = 85$ μK to values close to 40 μK [cf. Fig. 3(b)].

In order to calculate the ODT dynamics after termination of loading, we may complement Eq. (1) by two further equations describing the time evolution of the radial (T_{rad}) and axial (T_{ax}) temperatures

$$\dot{T}_{\mathrm{ax}} = -\frac{1}{3}\gamma_{\mathrm{ev}} N\left(\frac{T_{\mathrm{ev}}}{T} - 1\right) T_{\mathrm{ax}} - \frac{2}{3}\gamma_{\mathrm{rel}}\Delta T + \frac{4}{3}\gamma_{\mathrm{sc}} T_{\mathrm{rec}},$$

$$\dot{T}_{\mathrm{rad}} = -\frac{1}{3}\gamma_{\mathrm{ev}} N\left(\frac{T_{\mathrm{ev}}}{T} - 1\right) T_{\mathrm{rad}} + \frac{1}{3}\gamma_{\mathrm{rel}}\Delta T + \frac{2}{3}\gamma_{\mathrm{sc}} T_{\mathrm{rec}}. \quad (2)$$

Here, $T \equiv (T_{\mathrm{ax}} + 2T_{\mathrm{rad}})/3$, $\Delta T \equiv T_{\mathrm{ax}} - T_{\mathrm{rad}}$, $k_B T_{\mathrm{ev}}$ is the energy removed per evaporated particle, $k_B T_{\mathrm{rec}}$ is the photon recoil energy, γ_{sc} is the photon scattering rate of the ODT ($9\ \mathrm{s}^{-1}$), γ_{ev} is the evaporation loss parameter of Eq. (1), and γ_{rel} is the cross-dimensional relaxation (CR) rate. In Eq. (2), exponential thermalization of T_{rad} and T_{ax} is assumed, proven to be a suitable approximation in numerous previous CR studies [20,25,26]. According to Ref. [27], the CR rate is connected to the collision parameter γ_{rel} used in the context of Eq. (1) by the relation $\gamma_{\mathrm{rel}} = c_{\mathrm{rel}}\gamma_{\mathrm{coll}} N$ with a constant c_{rel} depending on the exact model of the scattering cross section. In the case of a temperature independent scattering cross section, $c_{\mathrm{rel}} = 2/5$ is predicted, while our experimental data are best reproduced for $c_{\mathrm{rel}} = 1/11$. The value of T_{ev} is obtained from the detailed balance model [24] used in the context of Eq. (1) as $k_B T_{\mathrm{ev}} = U_0(\eta^3 + 3\eta^2 + 6\eta + 6)/(\eta^3 + 2\eta^2 + 2\eta)$. Using the same initial axial and radial temperatures ($T_{\mathrm{ax},0} = 300$ μK, $T_{\mathrm{rad},0} = 85$ μK) and the value of σ_0/v_0 as in the calculated graphs of Figs. 2(b) and 2(c), the system of Eq. (1) with $R(P) = \gamma_B(P) = 0$ and Eq. (2) is solved numerically. As done in Fig. 2(b) for $\bar{N}$, we finally scale the calculated values for N by the calibration factor 0.53. The results for N and T_{rad} [solid lines in (a) and (b)] are shown in Fig. 3. Our calculations also provide the evolution of the axial temperature, [dashed line in Fig. 3(b)], which cannot be observed in our experiment. Within the validity range of the harmonic approximation, this lets us obtain the phase space density of $N\hbar^3\Omega_{\mathrm{ax}}\Omega_{\mathrm{rad}}^2/(k_B T)^3$ [shown as the dashed-dotted line in Fig. 3(b)], where $\Omega_{\mathrm{ax}} = 2\pi \times 20.3$ Hz and $\Omega_{\mathrm{rad}} = 2\pi \times 3.8$ kHz are the calculated axial and radial harmonic frequencies of the ODT.

We are aware of the fact that our model involves a number of distinct simplifications as the harmonic approximation of the ODT potential or the use of an average temperature for evaluating the evaporation loss parameter γ_{ev}. Nevertheless, its predictions are in good agreement with the observations. The adjustment of only three fit parameters ($\gamma_{B,0}, R_0, \sigma_0/v_0$) permits us to model the dependence of the loading dynamics on the pump power encoded in the functions $R(P)$, $\tau(P)$, and $\bar{N}(P)$. The adjustment of one additional parameter (c_{rel}) also yields a decent description of the decay dynamics including a correct prediction of the final radial temperature and particle number. This shows that the model, despite its simplifications, identifies the relevant physical mechanisms. It provides the useful insights that the loading mechanism is energy selective with respect to the radial degrees of freedom and that it is mainly limited by evaporation.

Finally, Fig. 4 indicates how an ODT could be continuously loaded with $^3P_0$ atoms. This state could play a central

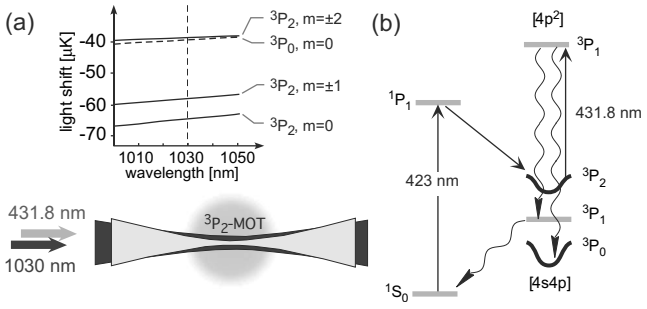

FIG. 4. Continuous loading scheme for an ODT of $^3P_0$ atoms. (a) Light shifts and sketch of beam configuration. (b) Relevant electronic levels.

role in future optical clocks exceeding 10^{-17} relative precision [14]. A dipole trap using 1030 nm light (readily available with sufficient power) produces nearly equal light shifts for $^3P_2$, $m=\pm 2$ and $^3P_0$, $m=0$ atoms, [cf. Fig. 4(a)]. Optical pumping between these states is achieved by means of 431.8 nm radiation coupling $[4s4p]^3P_2$ to $[4p^2]^3P_0$, [cf. Fig. 4(b)], which (apart from ppm contributions) decays either to $[4s4p]^3P_1$ or $[4s4p]^3P_0$ with a branching ratio of 44 to 56%. Both the triplet MOT and the singlet MOT are kept active during the entire loading. Atoms transferred to $[4s4p]^3P_1$ subsequently decay to $^1S_0$ and are thus readily transferred back to the cold $^3P_2$ reservoir.

In summary, we have shown that spatially selective optical pumping can be used for efficient continuous loading of $^1S_0$ calcium atoms into an optical dipole trap. Capture rates of up to 10^7 s^{-1} and phase space densities close to 4×10^{-5} are obtained. As compared to the start ensemble of precooled $^3P_2$ atoms, this amounts to an increase of the phase space density by nearly 10^3. Similar schemes should be applicable to many cases of interest, where conventional loading techniques are not available. We have briefly outlined the example of calcium atoms in the $^3P_0$ state, which could be a useful tool for time metrology.

ACKNOWLEDGMENTS

This work has been supported by DFG (Priority Program SPP 1116, He2334/9-1). C. Y. Yang acknowledges additional support from DAAD.

[1] S. A. Diddams *et al.*, Science **306**, 1318 (2004).
[2] J. Weiner *et al.*, Rev. Mod. Phys. **71**, 1 (1999).
[3] K. Burnett *et al.*, Nature (London) **416**, 225 (2002).
[4] J. Anglin and W. Ketterle, Nature (London) **416**, 211 (2002).
[5] H. Katori, T. Ido, Y. Isoya, and M. Kuwata-Gonokami, Phys. Rev. Lett. **82**, 1116 (1999).
[6] T. Binnewies, G. Wilpers, U. Sterr, F. Riehle, J. Helmcke, T. E. Mehlstaubler, E. M. Rasel, and W. Ertmer, Phys. Rev. Lett. **87**, 123002 (2001).
[7] E. A. Curtis, C. W. Oates, and L. Hollberg, Phys. Rev. A **64**, 031403(R) (2001); E. A. Curtis *et al.*, J. Opt. Soc. Am. B **20**, 977 (2003).
[8] J. Grünert and A. Hemmerich, Phys. Rev. A **65**, 041401(R) (2002).
[9] D. Hansen, J. Mohr, and A. Hemmerich, Phys. Rev. A **67**, 021401(R) (2003).
[10] Y. Takasu, K. Honda, K. Komori, T. Kuwamoto, M. Kumakura, Y. Takahashi, and T. Yabuzaki, Phys. Rev. Lett. **90**, 023003 (2003).
[11] T. H. Loftus, T. Ido, A. D. Ludlow, M. M. Boyd, and J. Ye, Phys. Rev. Lett. **93**, 073003 (2004).
[12] N. Poli, R. E. Drullinger, G. Ferrari, J. Leonard, F. Sorrentino, and G. M. Tino, Phys. Rev. A **71**, 061403(R) (2005).
[13] J. Helmcke *et al.*, IEEE Trans. Instrum. Meas. **52**, 250 (2003); C. Degenhardt *et al.*, Phys. Rev. A **72**, 062111 (2005).
[14] A. V. Taichenachev, V. I. Yudin, C. W. Oates, C. W. Hoyt, Z. W. Barber, and L. Hollberg, Phys. Rev. Lett. **96**, 083001 (2006); Z. W. Barber, C. W. Hoyt, C. W. Oates, L. Hollberg, A. V. Taichenachev, and V. I. Yudin, *ibid.* **96**, 083002 (2006).
[15] P. G. Mickelson, Y. N. Martinez, A. D. Saenz, S. B. Nagel, Y. C. Chen, T. C. Killian, P. Pelligrini, and R. Cote, Phys. Rev. Lett. **95**, 223002 (2005).
[16] O. Allard *et al.*, Eur. Phys. J. D **26**, 155 (2003); C. Degenhardt, T. Binnewies, G. Wilpers, U. Sterr, F. Riehle, C. Lisdat, and E. Tiemann, Phys. Rev. A **67**, 043408 (2003); F. Vogt *et al.*, Eur. Phys. J. D **44**, 73 (2007).
[17] J. P. Gordon and A. Ashkin, Phys. Rev. A **21**, 1606 (1980); S. Chu, J. E. Bjorkholm, A. Ashkin, and A. Cable, Phys. Rev. Lett. **57**, 314 (1986).
[18] P. Desbiolles and J. Dalibard, Opt. Commun. **132**, 540 (1996); H. Gauck, M. Hartl, D. Schneble, H. Schnitzler, T. Pfau, and J. Mlynek, Phys. Rev. Lett. **81**, 5298 (1998).
[19] A. Brusch, R. LeTargat, X. Baillard, M. Fouche, and P. Lemonde, Phys. Rev. Lett. **96**, 103003 (2006).
[20] D. Hansen and A. Hemmerich, Phys. Rev. Lett. **96**, 073003 (2006).
[21] T. P. Dinneen, K. R. Vogel, E. Arimondo, J. L. Hall, and A. Gallagher, Phys. Rev. A **59**, 1216 (1999).
[22] D. Hansen and A. Hemmerich, Phys. Rev. A **72**, 022502 (2005).
[23] J. Grünert and A. Hemmerich, Appl. Phys. B **73**, 815 (2001).
[24] W. Ketterle and N. van Druten, Adv. At., Mol., Opt. Phys. **37**, 181 (1996).
[25] C. R. Monroe, E. A. Cornell, C. A. Sackett, C. J. Myatt, and C. E. Wieman, Phys. Rev. Lett. **70**, 414 (1993).
[26] S. A. Hopkins, S. Webster, J. Arlt, P. Bance, S. Cornish, O. Marago, and C. J. Foot, Phys. Rev. A **61**, 032707 (2000); M. Arndt, M. BenDahan, D. Guery-Odelin, M. W. Reynolds, and J. Dalibard, Phys. Rev. Lett. **79**, 625 (1997); P. O. Schmidt, S. Hensler, J. Werner, A. Griesmaier, A. Gorlitz, T. Pfau, and A. Simoni, *ibid.* **91**, 193201 (2003); P. Spoden, M. Zinner, N. Herschbach, W. J. vanDrunen, W. Ertmer, and G. Birkl, *ibid.* **94**, 223201 (2005).
[27] G. M. Kavoulakis, C. J. Pethick, and H. Smith, Phys. Rev. A **61**, 053603 (2000).